ACS APPLIED MATERIALS & INTERFACES

Research Article

www.acsami.org

Ethylene Glycol Intercalated Cobalt/Nickel Layered Double Hydroxide Nanosheet Assemblies with Ultrahigh Specific Capacitance: Structural Design and Green Synthesis for Advanced Electrochemical Storage

Changhui Wang,[‡,†] Xiong Zhang,[†] Zhongtang Xu,[†] Xianzhong Sun,[†] and Yanwei Ma*[,†]

[†]Institute of Electrical Engineering, Chinese Academy of Sciences, Beijing 100190, China

[‡]University of Chinese Academy Sciences, Beijing 100049, China

Supporting Information

ABSTRACT: Because of the rapid depletion of fossil fuels and severe environmental pollution, more advanced energy-storage systems need to possess dramatically improved performance and be produced on a large scale with high efficiency while maintaining low-enough costs to ensure the higher and wider requirements. A facile, energy-saving process was successfully adopted for the synthesis of ethylene glycol intercalated cobalt/nickel layered double hydroxide (EG-Co/Ni LDH) nanosheet assembly variants with higher interlayer distance and tunable transitional-metal composition. At an optimized starting Co/Ni ratio of 1, the nanosheet assemblies display a three-dimensional, spongelike network, affording a high specific surface area with advantageous mesopore structure in 2−5 nm containing large numbers of about 1.2 nm micropores for promoting electrochemical reaction. An unprecedented electrochemical performance was achieved, with a specific capacitance of 4160 F g^{-1} at a discharge current density of 1 A g^{-1} and of 1313 F g^{-1} even at 50 A g^{-1}, as well as excellent cycling ability. The design and optimization of EG-Co/Ni LDH nanosheets in compositions, structures, and performances, in conjunction with the easy and relatively "green" synthetic process, will play a pivotal role in meeting the needs of large-scale manufacture and widespread application for advanced electrochemical storage.

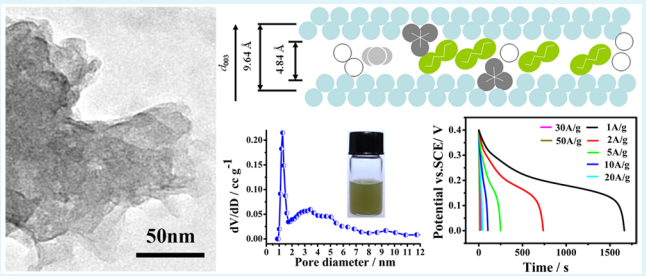

KEYWORDS: *electrochemical storage, layered double hydroxide, nanosheet assemblies, intercalation, nanostructure*

1. INTRODUCTION

The rapid depletion of fossil fuels and severe environmental pollution require society to move toward clean sustainable and renewable resources. More advanced energy-storage systems are starting to play a larger part in our lives, such as lithium-ion batteries, electrochemical capacitors, and solar energy conversion. We need to improve their performance substantially to meet the higher and wider requirements in today's mobile society.[1−3] The performance of such energy-storage devices is largely determined by the properties of the active electrode materials, which, in turn, are influenced by a number of physicochemical properties (e.g., composition, structure, and morphology).[4] The challenge as it stands now is what compositional, structural, and morphological materials we will use to optimize the electrochemical properties and how they can be produced on a large scale with high efficiency while still maintaining low-enough costs to ensure their worldwide adoption.[5]

Compositionally, the hydroxide of nickel crystallizes as a layered structure in two different polymorphic modifications, namely, β- and α-$Ni(OH)_2$. β-$Ni(OH)_2$ is a stoichiometric compound with the formula $Ni(OH)_2$ and is isostructural with the mineral brucite, $Mg(OH)_2$, while α-$Ni(OH)_2$ is hydroxyl-deficient and consists of positively charged layers of composition $[Ni(OH)_{2-x}(H_2O)_x]^{x+}$ that intercalate anions in the interlayer region to restore charge neutrality.[6] α-$Ni(OH)_2$ tends to lose the original crystal-plane stacking structure and becomes the turbostratic-disordered structure.[2] α-phase $Ni(OH)_2$ and β-phase $Ni(OH)_2$ transform into γ-phase NiOOH and β-phase NiOOH, respectively, after full electrochemical charging.[3] α-$Ni(OH)_2$ with a turbostratic-disordered structure has a larger interlayer distance, which is capable of realizing a two-electron reaction via an electrochemical conversion between the α-$Ni(OH)_2(Ni^{2+})$/γ-$NiOOH(Ni^{4+})$ redox couple and is expected to have a much higher specific capacity than commercialized β-$Ni(OH)_2$. The γ phase has a higher interlayer spacing, which leads to extensive swelling and subsequent breakdown of the β-$Ni(OH)_2$ electrode. On the other hand, the α-hydroxide and γ-oxyhydroxide phases have comparable

Received: April 15, 2015
Accepted: August 10, 2015
Published: August 10, 2015

DOI: 10.1021/acsami.5b03176
ACS Appl. Mater. Interfaces 2015, 7, 19601−19610

interlayer spacings. Thus, the oxidation of α-nickel hydroxide leads to oxyhydroxide without any mechanical failure.

Unfortunately, α-$Ni(OH)_2$ is thermodynamically unstable in a strong alkaline medium and easily transforms to β-$Ni(OH)_2$.[3] However, α-phase stabilization in an alkaline medium has been achieved by partial isomorphous substitution of nickel by other metal ions, resulting in the formation of layered double hydroxides (LDHs), which have exhibited stable reversible capacity.[6] Considerable research has demonstrated that the coincorporation of cobalt and nickel in the host layer can offer an effective way for achieving an improved electrochemical performance in comparison with monometallic hydroxides, not only by arresting the conversion of both α-nickel hydroxide to β-nickel hydroxide and α-$Co(OH)_2$ to Co_3O_4 in an alkaline medium but also by increasing the conductivity of α-$Ni(OH)_2$ electrode materials.[6−12] This can be validated by the investigations of $Co_{1-x}Ni_x$ hydroxide nanocones (NCs),[7] Co_xNi_{1-x} LDHs deposited on stainless steel electrodes,[8] nanostructured mesoporous Co_xNi_{1-x} LDHs,[10] etc.,[6] especially among which the highest specific capacitance of 2104 F g^{-1} at 1 A g^{-1} was obtained.[8] Composite cobalt/nickel hydroxides would be achieved via delamination and costacking,[6] microwave-assisted hydrothermal reaction,[7] potentiostatic deposition,[8] partial cation exchange,[9] chemical coprecipitation,[10,11] anodic deposition,[12] and so forth. While great effort has been made to develop various synthesis routes and to boost the electrochemical performances of cobalt/nickel hydroxides, many of the applications are largely restricted because the synthetic methodologies suffer high energy costs, an elevated temperature, complicated techniques, environmental pollution, or low yield, and the resulting product exhibits limited electrochemical properties[6−12] (see Table S1 for details).

Structurally, a key to reaching high capacitance is in using high-specific-surface-area (SSA) blocking and electronically conducting electrodes. It was also suggested that a well-balanced micro- or mesoporosity was needed to maximize the capacitance.[1] LDHs are a class of ionic lamellar compounds made up of positively charged rigid brucite-like layers with an interlayer region containing loosely attracted charge-compensating anions and solvation molecules.[2,13] The metal cations occupy the centers of an edge-sharing octahedral, whose vertexes contain hydroxide ions that connect to form infinite two-dimensional sheets. Nanosheets can not only increase the specific area of materials but also decrease remarkably the diffusion distance for ions from the bulk electrolyte to the surface of the active material owing to their very thin thickness on the scale of nanometers.[2] A range of functional nanosheet assemblies and their related materials in thin flay form as porous aggregates have displayed disorganized microtextures and novel properties, including their well-retained and inherited characteristics from the original nanosheets by selecting or chemically designing the right building block.[2,14] It is rather remarkable that the incorporation of organic molecules into inorganic layered hosts in general has presented an effective approach to obtaining novel nanocomposites with optimum pore sizes. Intercalated species are anchored to the clay layers, and their distribution yields channels and two-dimensional galleries providing a microporous structure that can be tailored by the nature and size of the intercalated species. The resulting solids have higher interlayer distances, and the potential application of organo-LDHs as new modified electrodes has been investigated.[15,16] In addition, intercalation reactions can be used as a low-temperature (chimie douche) method to prepare unique materials that may not be accessible by other techniques.[17] Despite the various advantages of the structure and synthetic techniques, few optimal organo-LDHs have been found as active electrode materials for energy storage to meet the current requirement, which can be achieved via a facile scale-up, low-cost, environmentally friendly technique and possess excellent electrochemical performances.[2,15] For example, dodecylsulfate-intercalated α-nickel and cobalt hydroxides (DS-Ni/Co) were obtained by delamination and costacking, and the resultant product underwent a 15 day anion-exchange process to obtain the end product, a nitrate-intercalated composite, in spite of the fact that it showed a reversible discharge capacity of 373 mAh g^{-1} in the first cycles and 340 mAh g^{-1} after 20 cycles.[6] Recently, DS-Co/Ni hydroxide (H) NCs, prepared via a microwave-assisted hydrothermal reaction, were directly used as supercapacitor electrode materials,[7] which displayed a highest specific capacitance of 1580 A g^{-1} at a galvanic current density of 10 A g^{-1} by control of the composition. Still, there exists a long run in the research on the organo-LDH electrode materials for energy storage, such as exploration of the facile scale-up and green synthetic techniques and optimization of the electrochemical properties to meet the needs of large-scale manufacture and widespread application.

More recently, we discovered that nanostructured α-$Co(OH)_2$ and α-$Ni(OH)_2$ LDHs, as a precursor to the $NiCo_2O_4$ spinel with a high electrochemical performance, can be obtained by a facile, one-step coprecipitation technique at a starting Co/Ni ratio of 2 via the introduction of a traditional aqueous system into an organic phase with ethylene glycol (EG) as the surfactant at room temperature.[18] Considering that EG is also extensively used as an intercalating agent,[19−26] if EG can be incorporated into the transition-metal rigid layers and, furthermore, if the ratios of Co/Ni of the host layers and structures and the morphologies of the products can be tunable in the fabrication process, it is promising to engineer an optimal EG-intercalated Co/Ni (EG-Co/Ni) LDH electrode material with high SSA, desirable porosity, and excellent electrochemical performances for advanced energy storage.[15]

In this work, the facile, one-step "bottom-up", energy-saving process was successfully adopted for the synthesis of a series of EG-Co/Ni LDH nanosheet assemblies with higher interlayer distance and tunable transitional-metal composition by adjusting the starting ratios of Co/Ni. As expected, the EG-Co/Ni LDH nanosheet assemblies' variants showed controllable structures, morphologies, and electrochemical properties. Remarkably, at an optimized starting Co/Ni ratio of 1, the nanosheet assemblies of the building blocks display a three-dimensional, spongelike network, affording a high SSA with advantageous mesopore structure in 2−5 nm containing large numbers of about 1.2 nm micropores to increase the density of the active sites and accommodate the electrolyte for promoting fluid/solid reaction. Ultimately, an unprecedented electrochemical performance was achieved, with a specific capacitance of 4160 F g^{-1} at a discharge current density of 1 A g^{-1} and of 1313 F g^{-1} even at 50 A g^{-1}, as well as excellent cycling ability. Then, the design and optimization of EG-Co/Ni LDH nanosheets in compositions, structures, and performances, in conjunction with the easy and relatively "green" synthetic process, will play a pivotal role in meeting the needs of large-scale manufacture and widespread application for advanced electrochemical storage.

DOI: 10.1021/acsami.5b03176
ACS Appl. Mater. Interfaces 2015, 7, 19601−19610

2. EXPERIMENTAL SECTION

Preparation of EG-Co/Ni LDH Nanosheet Assemblies. $Ni(NO_3)_2{\cdot}6H_2O$ (≥98.0%), $Co(NO_3)_2{\cdot}6H_2O$ (≥99.0%), NaOH (≥96.0%), and EG (≥96.0%) were used as source materials without further purification. $Ni(NO_3)_2{\cdot}6H_2O$ (≥98.0%) and $Co(NO_3)_2{\cdot}6H_2O$ (≥99.0%) were first dissolved in 80 mL of deionized water with 20 mL of EG (≥96.0%). The ratios of Co/Ni were 3:1, 2:1, 1:1, 1:2, and 1:3, respectively, the total amount remaining 0.012 M Co and Ni. NaOH (0.026 M) was sonicated with 270 mL of EG to give a colorless solution (pH = 11.70). The above claret solution containing Co^{2+} and Ni^{2+} was then added dropwise to the EG solution containing NaOH at room temperature under constant high-speed stirring to give a pea-green thixotropic mixture (pH = 10.62), followed by stirring for a further 18 h to undergo Ostwald ripening. In the whole solution of the reaction, the amount of EG is 290 mL and that H_2O is 80 mL. The green powder of the product was obtained when the reaction mixture was centrifuged, washed, and dried at 80 °C. The green color of the products will become deeper with an increase of Ni in the starting ratios of Co/Ni.[18]

Preparation of A-Co/Ni H. Also, for comparison purposes, A-Co/Ni H was prepared without the addition of EG in the traditional precipitation process at a starting Co/Ni ratio of 1:1. The preparation of the A-CoNi H is the same as the above part 1, except that EG was not added.

3. RESULTS AND DISCUSSION

Figure 1 displays the X-ray diffraction (XRD) patterns of the products obtained at various starting ratios of Co/Ni. For the

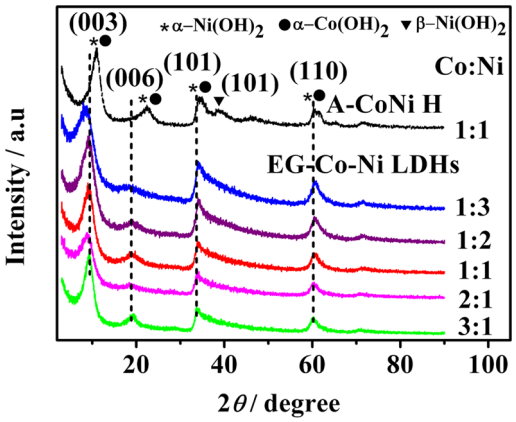

Figure 1. XRD patterns of EG-Co/Ni LDHs (solid) and A-Co/Ni H (dashed).

EG-Co/Ni LDHs, the reflections are fewer in number and more broadly indicative of poorly ordered samples with a typical layered structure. The strong peaks fall in the lower 2θ range and can be indexed as (003), (006), (101), and (110), respectively. A low-angle reflection appears at 9.64 Å (9.17°), followed by another reflection at about half of this spacing, 4.78 Å (18.95°). A third reflection appears at 2.62 Å (34.26°) and exhibits a pronounced asymmetry on the higher angle side. This feature is characteristic of turbostratic materials, in which the layers are stacked one upon another and randomly oriented about the principal (c) crystallographic axis.[8,27] All of these features match with the characteristic diffractions of both α-$Co(OH)_2$ and α-$Ni(OH)_2$ LDHs.[8,18] Another reflection of a similar line shape appears at 1.53 Å (60.46°). The (003) interlamellar distance (9.64 Å) increases compared to that (ca. 7.9 Å) of the A-Co/Ni H sample and the α-cobalt/nickel hydroxides reported in the literature.[6] A coherent shift of the (00l) peaks as a whole implies that the intercalation of EG is superior to that of the H_2O molecules in the "bottom-up" approach, taking into account the neutrality of the composition.[21] In addition, a typical scanning electron microscopy image of a cross section of the EG-Co/Ni LDH nanosheet assemblies also reveals the characteristics of a layered structure, which can be observed at the edge of the agglomerates (Figure S1).

For the A-Co/Ni H sample, the reflection at 38.45° can be seen from the (101) plane of the β-$Ni(OH)_2$ impurity.[11] In the organic–inorganic phase reaction system, the coprecipitation processes, nucleation, growth, and agglomeration, may be controlled by the EG addition, which can act as a buffer solvent of NaOH, a bidentate chelating agent of Ni^{2+} and Co^{2+}, and a stabilizing agent. The compositions, structures, and morphologies of the products will be governed over.[18]

The presence of the EG molecules in the new compounds was further examined by Fourier transform infrared (FT-IR) spectroscopy, as shown in Figures 2 and S2. In all of the

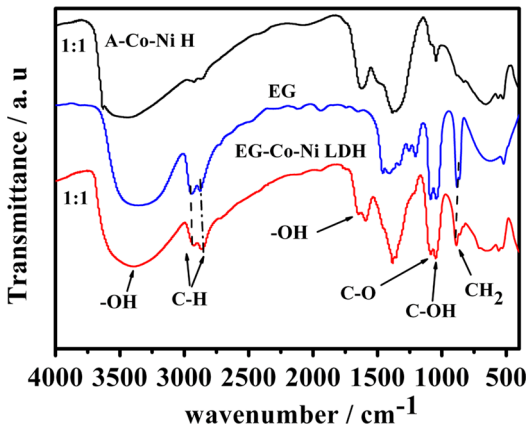

Figure 2. FT-IR spectra of EG and the samples EG-Co/Ni LDH and A-Co/Ni H prepared at a starting Co/Ni ratio of 1:1.

spectra, an intense and broad adsorption band at 3359–3436 cm^{-1} corresponds to the stretching vibration of hydrogen-bonded hydroxyl groups (ν_{O-H}) from all of the samples.[28−34] The O–H bending vibration of the interlayer H_2O is also observed at 1620–1650 and 1589–1596 cm^{-1} for the product A-Co/Ni H prepared at a starting ratio of 1:1 and all of the EG-Co/Ni LDHs, respectively. After all, part of H_2O can still intercalated into the layer of the samples because of the mixed reaction system of EG and H_2O. Moreover, the intensity of this peak varies from medium to weak, depending on the amount of H_2O in the as-prepared samples. We can see that there is the least H_2O in the EG-Co/Ni LDH prepared at a starting ratio of 1:1 of all of the samples from the weakest intensity of the peak of the bending vibration of OH. The O–H vibration peak position of 3359–3401 or 1589–1596 cm^{-1} possesses a lower wavenumber range for EG-Co/Ni LDHs or EG compared to that for A-Co/Ni H, which can be ascribed to the intercalation of EG in EG-Co/Ni LDHs. This might be caused by the decrease in the bond order between O and H when EG molecules exist in the samples.[35−37] One can see that the FT-IR spectra of EG-Co/Ni LDHs display the characteristic vibration bands of EG centered at ca. 2924 cm^{-1} (C–H antisymmetric stretching), ca. 2867 cm^{-1} (C–H symmetric stretching), ca.1085 cm^{-1} (C–O stretching), ca.1046 cm^{-1} (C–O–H bending), and ca.887 cm^{-1} (CH_2 rocking vibration) with a weak shoulder at 860 cm^{-1}.[28,29] The stretching vibrations of the

DOI: 10.1021/acsami.5b03176
ACS Appl. Mater. Interfaces 2015, 7, 19601–19610

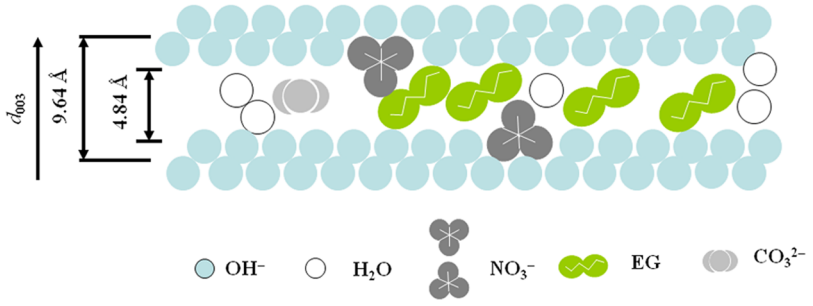

Figure 3. Schematic representation of the EG-Co/Ni LDH structure considering of a brucite-like hydroxide sheet with NO_3^-, EG, and H_2O molecules in the interlayer region.

C−H bonds shift toward lower frequency (2924 and 2867 cm^{-1}) with broader and weaker adsorption, while the CH_2 rocking vibration shifts to a higher wavenumber (ca. 887 cm^{-1}) with a weak shoulder for EG-Co/Ni LDHs, compared to the pure EG bands (2943, 2878, 883, and 864 cm^{-1}, respectively).[20,22] EG, with a nominal diameter of 4.2 Å, has been thought to be grafted into magnesium−aluminum hydrotalcite,[19] kaolinite,[23] bochmite,[24] gibbsite,[25] and zinc−aluminum double hydroxide[26] or be bounded to α-$Ni(OH)_2$ layers, with hydrotalcite-like structure.[21] Meanwhile, the IR spectra with clear shift or splitting were also observed compared to pure EG.[19,21,22] Among of them, the clear shifts of the C−H adsorption peaks in magnesium−aluminum hydrotalcite were attributed to dense packing of the EG molecules and the close interaction of the OH groups in EG with the interlayer components.[19] It has been accepted that the nature of the C−H stretching adsorption band (strong peaks at 2850−2950 cm^{-1}) suggests that the alkyl chains take up an all-trans conformation, and if the chains were disordered, the peak at 2920 cm^{-1} would be broad and weak.[29] Meanwhile, intensive research has found that the bands caused by the CH_2 rocking vibration have blue shifts when EG is intercalated between inorganic layers, such as in bochmite,[24] a Zn−Al−Co_3 LDH compound.[25,26]

The components and arrangement of the intercalated species in the intergallery have been investigated by considering the interlayer distances or the intergallery heights for the deviates of the hydroxide layered compounds.[21,22,35] The intergallery heights were calculated by subtracking the thickness of the brucite-like layer (0.48 nm) from the basal reflex d_{003} value of the hydrotalcite-like samples.[19,35] For EG-intercalated hydroxide layered compounds, a number of researchers have found that the expansion of intergallery heights to within the range from 0.36 nm to values close to the EG diameter (0.42 nm) was the result of intercalation of monolayer EG molecules, while the range from 0.84 nm to approximately the sum of two of those was one bilayer of EG molecules, which can possess a horizontal, tilt, or zigzag-like arrangement.[19,21,22] α-Cobalt hydroxide is isostructural with α-nickel hydroxide, and when the layers of α-nickel hydroxide are interspersed with the layers from an isostructural layered solid, α-cobalt hydroxide, the resulting α-cobalt/nickel hydroxides are structurally similar to hydrotalcite-type LDHs. Therefore, the generic formula for the LDHs may be written as $[M^{2+}_{1-x}M^{2+}_x(OH)_{2-y}][A^{z-}]_{y/z}\cdot mH_2O$, similarly, where A^{z-} is a nonframework charge-compensating inorganic or organic anion and M may be written as Ni^{2+} and Co^{2+}, respectively. That is, the Co/Ni LDHs consist of positively charged layers, and anions or molecules containing electronegative groups, such as O−H, can be intercalated by electrostatic interaction. EG is a neutralized molecule, but it contains the electronegative O−H group. As a result, EG can intercalate into the Co/Ni LDH by electrostatic interaction between their O−H and the positively charged layers of composition Co/Ni LDH. Moreover, the intercalation of EG is superior to that of H_2O from the results of the XRD (Figure 1) and FT-IR (Figures 2 and S2). For the current EG-Co/Ni LDHs, the interlayer distances (d_{003}) of ca. 9.64 Å correspond to intergallery height of ca. 4.84 Å, assuming 4.8 Å as the thickness of the brucite-like layer.[19,35] In the case of the EG-Co/Ni LDH nanosheet assemblies, we can draw the conclusion that EG was intercalated and chemically bonded to the cobalt/nickel hydroxide layers with adoption of a "tilled" position within the gallery (Figure 3) with respect to the layer plane.[21,22]

The existence and nature of the charge-compensating anions can also be investigated with FT-IR spectroscopy. The intense band at 1384 cm^{-1} in the spectra of EG-Co/Ni LDHs and A-Co/Ni H corresponds to the ν_3 mode of NO_3^-.[35−39] The adsorbance at ca. 1356 cm^{-1} indicates the existence of a small amount of CO_3^{2-} (ν_{C-O}), which is due to the unavoidable adsorption of CO_2 by the basic solution.[13,33,40] From the XRD pattern of A-Co/Ni H (Figure 1), one can observe that the introduction of additional CO_3^{2-} to the interlayer space has almost no effect on the expansion of the interlayer distances of EG-Co/Ni LDHs, as reported by other researchers in the literature.[22] Additionally, the broader bands in the range 646−668 cm^{-1} and the peaks at ca. 560 cm^{-1} with a shoulder at ca. 525 cm^{-1} are assigned to the δ_{M-O-H} and ν_{M-O} vibrations, respectively, where M = Co and Ni.[30−33]

As shown in Figure 3, therefore, there are charge-compensating anions of NO_3^-, a small amount of CO_3^{2-}, and neutralized molecules EG and H_2O between the gallery of the Co/Ni LDH. Ultimately, we can achieve EG-Co/Ni LDHs with enlarged interlamellar distances.

According to the collected data (Table 1) from the energy-dispersive X-ray spectroscopy (EDS) of the samples, the atomic

Table 1. EDS Analysis of Cobalt and Nickel in EG-Co/Ni LDHs and A-Co/Ni H

starting molar ratio (Co/Ni)	Co (atom %)	Ni (atom %)	elemental composition
3:1[a]	22.39	7.98	EG-Co_3/Ni LDH
2:1[a]	11.65	5.93	EG-Co_2/Ni LDH
1:1[a]	8.92	8.90	EG-Co/Ni LDH
1:2[a]	2.90	5.80	EG-Co/Ni_2 LDH
1:3[a]	2.59	8.76	EG-Co/Ni_3 LDH
1:1[b]	11.66	11.65	A-Co/Ni H

[a]An EG and H_2O system. [b]A pure H_2O system.

DOI: 10.1021/acsami.5b03176
ACS Appl. Mater. Interfaces 2015, 7, 19601−19610

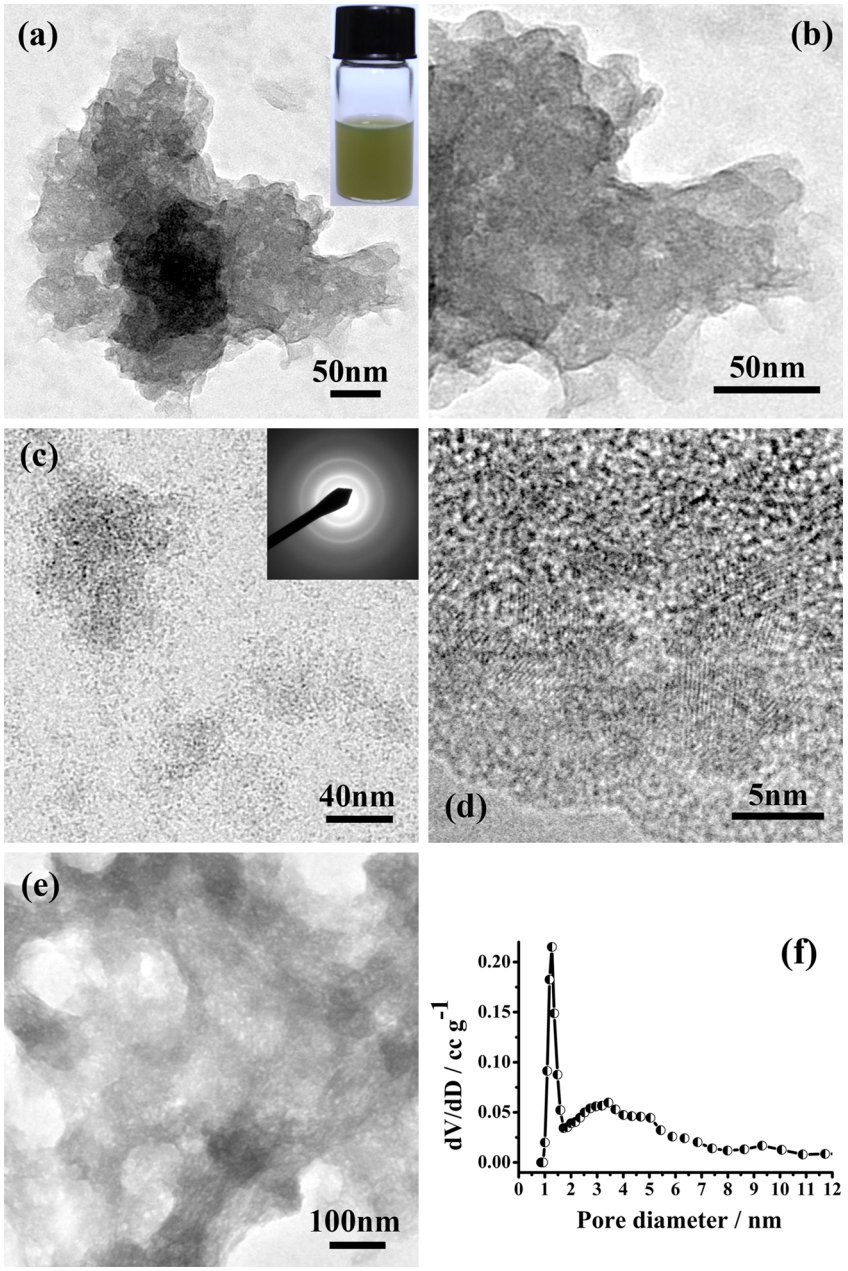

Figure 4. (a) TEM and digital image (inset). (b and e) TEM images. (c) TEM image with the corresponding SAED pattern in the upper right inset. (d) High-resolution TEM image of the EG-Co/Ni LDH nanosheets. (f) Pore-size distribution of the EG-Co/Ni LDH nanosheet assemblies using the NLDFT algorithm.

ratios of Co/Ni in the composite are in good agreement with the starting ratios of Co/Ni, respectively. Consequently, a series of EG-Co/Ni LDH nanosheet assemblies with extended interlayer spacing of ca. 9.64 Å and tunable transitional-metal composition were successfully synthesized as a new class of hybrid material through the facile, one-step, "bottom-up", energy-saving process at different starting ratios of Co/Ni.

The inherent structural and morphological characteristics of EG-Co/Ni LDHs are shown as transmission electron microscopy (TEM) images (Figures 4a–e and 5a–d). For the EG-Co/Ni LDH sample, the assembled nanosheets reveal a three-dimensional, roselike appearance and the layering is evident from the aggregates of thin crimpled nanosheets without definite shape at the edge (Figure 4a,b). The ultrathin nature of the nanosheets can be qualitatively conceived from the very faint contrast of the nanosheets lying on the grid (Figure 4c).[2] The boundary of the nanosheets is not obvious because of the weak crystallinity (Figure 4c,d). The edge length is most likely 50–100 nm in both dimensions (Figure 4c), and ca. 5 nm nanoparticle-like ultrathin nanosheets can also be seen (Figure 4d) because of the weak crystallinity. At the same time, the diffused halo of the selected-area electron diffraction (SAED) pattern in the inset of Figure 4c further indicates the poor crystallinity and polycrystalline characteristics of the sample. Upon close examination, one can recognize the mesopores (Figure 4a,b,d) and micropores (Figure 4d) of the nanosheet assemblies. Finally, the nanosheets will further stack into loose, spongelike large blocks without specific morphology and give a porous microstructure (Figure 4e). The interconnected three-dimensional porous inorganic networks

DOI: 10.1021/acsami.5b03176
ACS Appl. Mater. Interfaces 2015, 7, 19601–19610

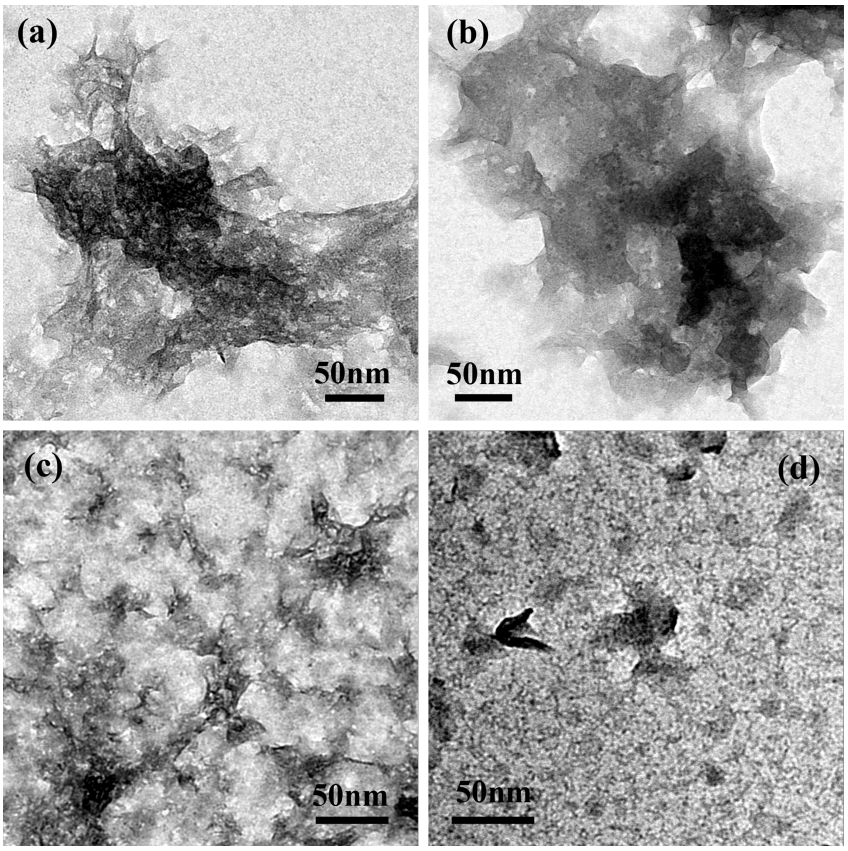

Figure 5. TEM images of (a) EG-Co/Ni_2 LDH, (b) EG-Co_2/Ni LDH, (c) EG-Co/Ni_3 LDH, and (d) EG-Co_3/Ni LDH nanosheets.

will not only facilitate the penetration of electrolytes in the whole hydroxides but also shorten the proton diffusion distance, promoting fluid/solid reaction.[41]

Figure 4f displays the distribution of the nonlocal density functional theory (NLDFT) pore sizes from the corresponding N_2 adsorption/desorption isotherm. One can further observe that mesoporous EG-Co/Ni LDH nanosheet assemblies containing large numbers of micropores have been achieved. The majority of the pores include both micropores of 1.2 nm and mesopores of 3.5 and 5 nm, as well as a few of 9.3 nm, falling in the optimal sizes for supercapacitor applications.[1,42−44] Similar pore-size distributions have been found in cationic[45−47] and anionic pillared clays[48] and LDHs containing intercalated manganese oxide species.[35] They suggested that the first narrow peak is related to the longitudinal pore size (gallery height), while the broader peak at higher values represents the lateral pore size or interparticle void. Thus, we attribute the micropores and mesopores in the EG-Co/Ni LDH nanosheet assemblies to the longitudinal pores from the expanded gallery height and the lateral pores or interparticle void from the well assembling or stacking of nanosheets, respectively. From the isotherm, a Brunauer−Emmett−Teller (BET) SSA of 168 $m^2\ g^{-1}$ of the overall products was derived, with a Barrett−Joyner−Halenda pore volume of 0.1 $cm^3\ g^{-1}$. The coexistence of micro- and mesopores and the high BET SSA may be expected to have a good effect on the improvement of the electrochemical properties for the EG-Co/Ni LDH nanosheet assemblies as active electrode materials.[1]

When the compositional ratio of Co/Ni deviates from 1, the layered structures of the EG-Co/Ni LDH nanosheets can also be seen from the TEM images (Figure 5a−d), while there are many changes in the structure and morphology compared to that of the product EG-Co/Ni LDH. When the compositional ratio of Co/Ni or Ni/Co increases to 2, the layer nanosheets exhibit evident aggregates (Figure 5a,b), and, furthermore, for the EG-Co_2/Ni LDH sample, the average layer size and thickness become bigger and thicker (Figure 5b). When the compositional ratio of Co/Ni or Ni/Co reaches 3, the layer nanosheets turn into small fragments (Figure 5c,d) or further aggregate to thicker layered blocks as EG-Co/Ni_3 LDH sample displays (Figure 5d). The thickness of the layered structure of EG-Co/Ni LDHs was calculated by using the Debye−Scherrer formula according to their XRD data (Figure 1). As shown in Figure 6d, when the compositional ratios of Co/Ni are 1:2, 2:1, 1:1, 1:3, and 3:1, the thicknesses of the layered structures are 32.8, 40.2, 26.8, 30, and 46.6 Å, respectively. The variation trend of the values is almost consistent with the observation results from the TEM images (Figures 4 and 5).

From the TEM image of A-Co/Ni H (Figure S4), both the nanosheets and nanobelt can be evidently seen, and the nanobelts exhibit better crystallinity (Figure S5) than the EG-Co/Ni LDH nanosheets, consistent with the XRD results. The thickness of the layered structure of A-Co/Ni H is 31.4 Å, coming from the Debye−Scherrer formula. The microstructure affords a mesoporous structure, with the majority of pore sizes falling at 5 nm and with small micropores of ca. 1.5 nm (Figure S6) and a BET SSA of 60 $m^2\ g^{-1}$. Accordingly, the EG-Co/Ni LDH nanosheet variants with controlled structure can be obtained by tuning the composition and reaction system. The optimized EG-intercalated α-$Ni(OH)_2$/$Co(OH)_2$ (EG-Co/Ni LDH) possesses optimal microstructure for electrochemical

DOI: 10.1021/acsami.5b03176
ACS Appl. Mater. Interfaces 2015, 7, 19601−19610

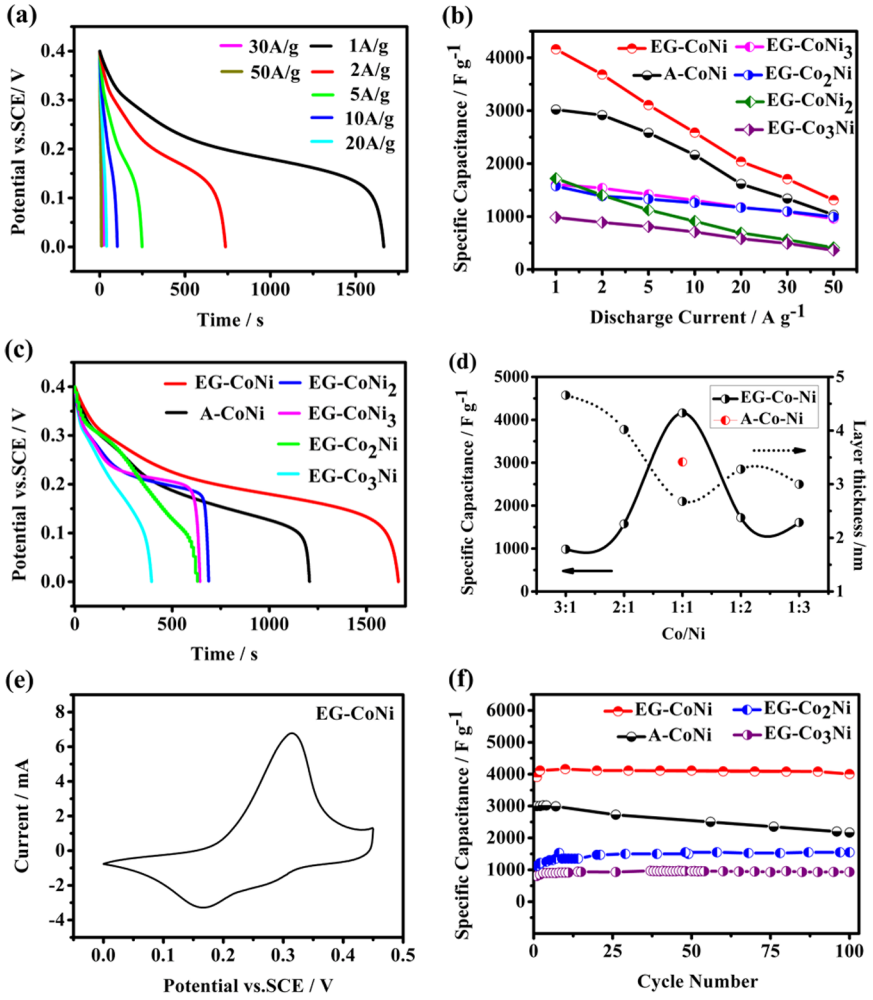

Figure 6. (a) Galvanostatic discharge curves at various discharge current densities of the EG-Co/Ni LDH nanosheet assemblies. (b) Average specific capacitance at various discharge current densities, (c) galvanostatic discharge curves at a current density of 1 A g^{-1}, and (d) average specific capacitance at a current density of 1 A g^{-1} (solid) for the EG-Co/Ni variants and A-Co/Ni H, and the thickness of the layered structure of EG-Co/Ni LDHs calculated by using the Debye−Scherrer formula (short dotted). (e) CV curves at a sweep rate of 5 mV s^{-1} of the EG-Co/Ni LDH nanosheet assemblies. (f) Stability test in terms of the specific capacitance at a current density of 1 A g^{-1} for samples EG-Co/Ni LDH, EG-Co_2/Ni LDH, EG-Co_3/Ni LDH, and A-Co/Ni H.

reaction, such as ultrathin nanosheets, enlarged interlayer space, increased BET SSA, and outstanding micro- and mesoporous structure.

The electrochemical behavior of EG-Co/Ni LDH nanosheet assemblies was investigated by galvanostatic charge−discharge and cyclic voltammetry (CV) as supercapacitor electrodes (see the Supporting Information for experimental details). Figure 6a shows galvanostatic discharge curves of the EG-Co/Ni LDH nanosheet assemblies at various current densities. We can find that there are voltage plateaus, which match well with the redox peaks in the CV curves (Figure 6e). They can be related to a combined effect of the following redox reactions: $Co(OH)_2 + OH^- \leftrightarrow CoOOH + H_2O + e^-$ and $Ni(OH)_2 + OH^- \leftrightarrow NiOOH + H_2O + e^-$, respectively.[7] The above phenomena indicate that the samples exhibit pseudocapacitance behavior, which is also similar to a battery-like material used for nickel-based batteries.[49] The background signal originating from nickel mesh substrates was almost negligible. Interestingly, as expected, compared to the other EG-Co/Ni LDHs with different metal compositions of cobalt and nickel, as well as the sample A-Co/Ni H (Figure 6c,d), the specific capacitance of the EG-Co/Ni LDH nanosheet assemblies has dramatically increased and reached a highest value of 4160 F g^{-1} (Figure 6a−d) at a discharge current density of 1 A g^{-1}, remaining steady at more than 96% after 100 cycles of charge and discharge at 1 A g^{-1} (Figure 6f). Besides, to our knowledge, the ultrahigh specific capacitance of the EG-Co/Ni LDH nanosheets is superior to that of any Co/Ni-based active electrode materials reported for energy storage so far.[10−12] More interestingly, the specific capacitance of the EG-Co/Ni LDH nanosheet assemblies is still as high as 1313 F g^{-1} even at a high discharge current density of 50 A g^{-1} (Figure 6a,b).

The unique nanostructure of the EG-Co/Ni LDH nanosheet assemblies is undoubtedly indispensable to the ultrahigh electrochemical performances. As shown in Figure 6d, the change trend of the thickness of the layered structure is almost opposite to that of the specific capacitance of the EG-Co/Ni LDHs. That is, the sample EG-Co/Ni LDH that possesses the least thickness (26.8 Å) of the layered structure has the highest specific capacitance (4160 F g^{-1}) and vice versa. This is because the ultrathin nanosheets can not only increase the specific area of the materials but also remarkably decrease the diffusion

DOI: 10.1021/acsami.5b03176
ACS Appl. Mater. Interfaces 2015, 7, 19601−19610

distance for ions from the bulk electrolyte to the surface of the active material.[2]

Specifically, the advantageous pore-size distribution plays a great role in the improved capacitance. First, the mesopores, which are larger than the size of two solvated ions of the electrolyte, provide a more favorable and quicker pathway for ions to penetrate, and the improved ionic mass transport inside mesopores leads to faster electrochemical reaction.[1] Second, despite the great quality of investigations on various mesoporous materials as electrode materials, only a moderate improvement in capacitance has been made, such as a specific capacitance of 1809 F g^{-1} for a mesoporous $Co_{0.41}/Ni_{0.59}$ LDH,[10] 2104 F g^{-1} for a potentiostatically deposited porous $Co_{0.72}/Ni_{0.28}$ LDH without micropores,[8] etc.[1] It was proposed that partial or complete removal of the salvation shell of ions could occur, allowing access to small pores (<2 nm) and leading to an improved capacitance.[1,44] As discussed before, an intercalation of EG superior to that of the H_2O molecules enlarges the interlayer space, and the larger spacing would provide easy access of OH^- ions (6−7.6 Å) and protons to α-$Co(OH)_2/Ni(OH)_2$ interlayer galleries. The enlarged interlayer space supplies an exceptional microporous structure (ca. 1.2 nm) for electrochemical reaction. Consequently, for the sample EG-Co/Ni LDH, the desolvated hydrated ions can diffuse into the micropore surfaces to meet more redox reaction. Then, an important capacitive contribution should come from the large numbers of micropores.[1,8,44]

On the other hand, the high BET SSA with excellent micro- and mesoporosity affords a high density of active sites to increase the redox reaction and ease mass transfer of the electrolyte.[2,42] Simultaneously, the interior hollow spaces coming from the loose, spongelike, three-dimensional network aggregates will decrease the mass-transfer resistance encountered in electrolyte penetration and ion diffusion and allow easier electron hopping between neighboring nanoparticles.[42] Hence, it may accommodate the volume change in the redox reaction and enhance the cyclability of the electrode material as a result.[40,50]

Additionally, as shown in Figure 6c, the EG-Co/Ni LDH nanosheet assemblies possess an increased discharge potential plateau, compared with the sample A-Co/Ni H. Considering that there are significant differences in the electronegativity between carbon (2.55) and cobalt (1.88) or nickel (1.92), we attribute this to changes of both the Madelung energy and the lattice covalency relating to the position of the Fermi level for the EG-Co/Ni LDH because of the probable charge transfer between the intercalated EG and the Co/Ni LDH.[51,52] The high specific capacity and discharge potential of EG-Co/Ni LDH make it suitable for battery applications.[3]

It is worth noting that the sample A-Co/Ni H displays a second highest specific capacitance of 3020 F g^{-1} (Figure 6b,d), while the decay is obvious and remains only 72% (2167 F g^{-1}) after 100 cycles at a discharge current density of 1 A g^{-1} (Figure 6f). Similarly, suitable 2−5 nm mesopores and 1.5 nm micropores should be the main contributions to the high capacity of A-Co/Ni H.[1,42,44] At the same time, fewer micropores and the lower BET SSA limit further improvement in the capacitance because of the lack of more active sites for electrochemical reaction in A-Co/Ni H.[1,2] Liu et al. have also found that $Co_{0.5}/Ni_{0.5}$ hydroxide NCs possess the highest specific capacitance in a series of cobalt/nickel hydroxide NCs and attributed the appearance of an enhancement of the electroactive sites participating in the redox reaction to possible valence interchange or charge hopping between cobalt and nickel cations.[7,8] It is not surprising that the metal (cobalt and nickel) composition ratio of 1 has helped to improve the specific capacitance in both the products EG-Co/Ni LDH and A-Co/Ni H. It also implies the importance of optimizing the metal composition in the enhancement of the electrochemical performance for EG-Co/Ni LDHs.

It is not inconceivable that one can achieve EG-intercalated α-$Co(OH)_2/Ni(OH)_2$ layered double hydroxides (EG-Co/Ni LDHs) without β-phase impurity when EG is introduced into the transitional aqueous phase. This will assure realization of a two-electron reaction via an electrochemical conversion between the α-$Ni(OH)_2(Ni^{2+})/\gamma$-$NiOOH(Ni^{4+})$ redox couple, after full electrochemical charging,[3] which will, in turn, make a great contribution to the increase of the specific capacitance of the EG-Co/Ni LDH nanosheet electrode material.

Moreover, all of the EG-Co/Ni LDH variants possess enhanced cycle stability, compared to the A-Co/Ni H sample (Figure 6f). We speculate that it mainly arises from the differences of the compositions, structures, and morphologies of the EG-Co/Ni LDHs from the A-Co/Ni H, including the enlarged interlayer spaces, possible existence of passivation of the unsatisfied Co−Ni dangling bond from the molecule of EG,[53] etc., which are useful to inhibit the decay in the specific capacitance. It can also be illustrated by their improved thermal stability from thermogravimetric analysis and differential scanning calorimetry analysis (TG-DSC) in air (see the Supporting Information for details), such as shown in Figure S8; a higher decomposition temperature was necessary for EG-Co/Ni LDH than that for A-Co/Ni H.

In brief, the above study confirms the feasibility of the design and optimization of the compositions, structures, and morphologies of EG-Co/Ni LDHs for dramatically improved electrochemical energy storage by control of the starting ratios of Co/Ni and adoption of the facile, one-step, "bottom-up", energy-saving approach.

4. CONCLUSION

In summary, EG-Co/Ni LDH nanosheet assemblies with unprecedented electrochemical performance were obtained through compositional, structural and morphological tuning, and successfully developing a facile, one-step, "bottom-up", energy-saving approach. The assemblies of the ultrathin nanosheets afford a three-dimensional, spongelike network, which provides a high BET SSA of 168 m^2 g^{-1} with 2−5 nm mesopore structure containing large numbers of 1.2 nm micropores. The unique microstructure has a great influence on easing the mass transfer, promoting the density of active sites and increasing the electrochemical reaction, and results in a superior specific capacitance of 4160 F g^{-1} at a discharge current density of 1 A g^{-1} and 1313 F g^{-1} even at 50 A g^{-1}, as well as excellent cycling ability. The design and optimization of EG-Co-Ni LDH nanosheets in compositions, structures, and performances, benefiting from the relatively "green" synthetic process, will provide an effective strategy to meet the needs of large-scale manufacture and widespread application for advanced electrochemical storage. This work can also open up the prospects for developing diverse advanced functional nanohybrid materials with required structures and performances for various potential applications.

DOI: 10.1021/acsami.5b03176
ACS Appl. Mater. Interfaces 2015, 7, 19601−19610

■ ASSOCIATED CONTENT

Supporting Information

The Supporting Information is available free of charge on the ACS Publications website at DOI: 10.1021/acsami.5b03176.

Details of characterization and electrochemical measurement of the as-prepared products and supplementary table, figures, and corresponding discussion (PDF).

■ AUTHOR INFORMATION

Corresponding Author

*E-mail: ywma@mail.iee.ac.cn.

Notes

The authors declare no competing financial interest.

■ ACKNOWLEDGMENTS

The authors are grateful for financial support from the National Natural Science Foundation of China (Grant 51472238).

■ REFERENCES

(1) Simon, P.; Gogotsi, Y. Materials for Electrochemical Capacitors. *Nat. Mater.* **2008**, *7*, 845−854.

(2) Wang, Q.; O' Hare, D. Recent Advances in the Synthesis and Application of Layered Double Hydroxide (LDH) Nanosheets. *Chem. Rev.* **2012**, *112*, 4124−4155.

(3) Gao, X. P.; Yang, H. X. Multi-Electron Reaction Materials for High Energy Density Batteries. *Energy Environ. Sci.* **2010**, *3*, 174−189.

(4) Hahn, B. P.; Long, J. W.; Rolison, D. R. Something from Nothing: Enhancing Electrochemical Charge Storage with Cation Vacancies. *Acc. Chem. Res.* **2013**, *46*, 1181−1191.

(5) Melot, B. C.; Tarascon, J.-M. Design and Preparation of Materials for Advanced Electrochemical Storage. *Acc. Chem. Res.* **2013**, *46*, 1226−1238.

(6) Nethravathi, C.; Ravishankar, N.; Shivakumara, C.; Rajamathi, M. Nanocomposites of α-Hydroxides of Nickel and Cobalt by Delamination and Co-Stacking: Enhanced Stability of α-Motifs in Alkaline. *J. Power Sources* **2007**, *172*, 970−974.

(7) Liu, X. H.; Ma, R. Z.; Bando, Y. S.; Sasaki, T. A General Strategy to Layered Transition-Metal Hydroxide Nanocones: Tuning the Composition for High Electrochemical Performance. *Adv. Mater.* **2012**, *24*, 2148−2153.

(8) Gupta, V.; Gupta, S.; Miura, N. Potentiostatically Deposited Nanostructured Co_xNi_{1-x}Layered Double Hydroxides as Electrode Materials for Redox-Supercapacitors. *J. Power Sources* **2008**, *175*, 680−685.

(9) Chen, W. H.; Yang, Y. F.; Shao, H. X.; Fan, J. Tunable Electrochemical Properties Brought About by Partial Cation Exchange in Hydrotalcite-Like Ni−Co/Co−Ni Hydroxide Nanosheets. *J. Phys. Chem. C* **2008**, *112*, 17471−17477.

(10) Hu, Z. A.; Xie, Y. L.; Wang, Y. X.; Wu, H. Y.; Yang, Y. Y.; Zhang, Z. Y. Synthesis and Electrochemical Characterization of Mesoporous Co_xNi_{1-x} Layered Double Hydroxides as Electrode Materials for Supercapacitors. *Electrochim. Acta* **2009**, *54*, 2737−2741.

(11) Wang, G. P.; Zhang, L.; Kim, J.; Zhang, J. J. Nickel and Cobalt Oxide Composite as a Possible Electrode Material for Electrochemical Supercapacitors. *J. Power Sources* **2012**, *217*, 554−561.

(12) Hu, C. C.; Cheng, C. Y. Ideally Pseudocapacitive Behavior of Amorphous Hydrous Cobalt-Nickel Oxide Prepared by Anodic Deposition. *Electrochem. Solid-State Lett.* **2002**, *5*, A43−A46.

(13) Lei, L. X.; Hu, M.; Gao, X. R.; Sun, Y. M. The Effect of the Interlayer Anions on the Electrochemical Performance of Layered Double Hydroxide Electrode Materials. *Electrochim. Acta* **2008**, *54*, 671−676.

(14) Ma, R. Z.; Sasaki, T. Nanosheets of Oxides and Hydroxides: Ultimate 2D Charge-Bearing Functional Crystallite. *Adv. Mater.* **2010**, *22*, 5082−5104.

(15) Newman, S. P.; Jones, W. Syntesis, Characterization and Applications of Layered Double Hydroxides Containing Organic Guests. *New J. Chem.* **1998**, *22*, 105−115.

(16) Ruiz-Hitzky, E.; Aranda, P.; Belver, C. In *Manipulation of Nanoscale Materials*; Ariga, K., Ed.; The Royal Society of Chemistry: London, 2012; Chapter 4, pp 87−111.

(17) Khan, A. I.; O'Hare, D. Intercalation Chemistry of Layered Double Hydroxides: Recent Developments and Applications. *J. Mater. Chem.* **2002**, *12*, 3191−3198.

(18) Wang, C. H.; Zhang, X.; Zhang, D. C.; Yao, C.; Ma, Y. W. Facile and Low-Cost Fabrication of Nanostructured $NiCo_2O_4$ Spinel with High Specific Capacitance and Excellent Cycle Stability. *Electrochim. Acta* **2012**, *63*, 220−227.

(19) Stanimirova, T.; Hibino, T. Ethylene Glycol Intercalation in $MgAlCO_3$ Hydrotalcite and Its Low-Temperature Intermediate Phases. *Appl. Clay Sci.* **2006**, *31*, 65−75.

(20) Tunney, J. J.; Detellier, C. Preparation and Characterization of Two Distinct Ethylene Glycol Derivatives of Kaolinite. *Clays Clay Miner.* **1994**, *42*, 552−560.

(21) Kasai, A.; Fujihara, S. Layered Single-Metal Hydroxide/Ethylene Glycol as a New Class of Hybrid Material. *Inorg. Chem.* **2006**, *45*, 415−418.

(22) Li, Y.; Xie, X. W.; Liu, J. L.; Cai, M.; Rogers, J.; Shen, W. J. Synthesis of α-$Ni(OH)_2$ with Hydrotalcite-like Structure: Precursor for the Formation of NiO and Ni Nanomaterials with Fibrous Shapes. *Chem. Eng. J.* **2008**, *136*, 398−408.

(23) Tunney, J.; Detellier, C. Preparation and Characterization of an 8.4 Å Hydrate of Kaolinite. *Clays Clay Miner.* **1994**, *42*, 473−476.

(24) Inoue, M.; Kominami, H.; Kondo, Y.; Inui, T. Organic Derivatives of Layered Inorganics Having the Second Stage Structure. *Chem. Mater.* **1997**, *9*, 1614−1619.

(25) Inoue, M.; Kondo, Y.; Inui, T. An Ethylene Glycol Derivative of Boehmite. *Inorg. Chem.* **1988**, *27*, 215−221.

(26) Guimaraes, J. L.; Marangoni, R.; Ramos, L. P.; Wypych, F. Covalent Grafting of Ethylene Glycol into the Zn−Al−CO_3 Layered Double Hydroxide. *J. Colloid Interface Sci.* **2000**, *227*, 445−451.

(27) Rajamathi, M.; Kamath, P. V.; Seshadri, R. Chemical Synthesis of a-Cobalt Hydroxide. *Mater. Res. Bull.* **2000**, *35*, 271−278.

(28) Wang, D. Y.; Das, A.; Costa, F. R.; Leuteritz, A.; Wang, Y. Z.; Wagenknecht, U.; Heinrich, G. Synthesis of Organo Cobalt-Aluminum Layered Double Hydroxide via a Novel Single-Step Self-Assembling Method and Its Use as Flame Retardant Nanofiller in PP. *Langmuir* **2010**, *26*, 14162−14169.

(29) Nethravathi, C.; Rajamathi, M.; Ravishankar, N.; Basit, L.; Felser, C. Synthesis of Graphene Oxide-Intercalated α-Hydroxides by Metathesis and Their Decomposition to Graphene/Metal Oxide Composites. *Carbon* **2010**, *48*, 4343−4350.

(30) Roginskaya, Y. E.; Morozova, O. V.; Lubnin, E. N.; Ulitina, Y. E.; Lopukhova, G. V.; Trasatti, S. Characterization of Bulk and Surface Composition of $Co_xNi_{1-x}O_y$ Mixed Oxides for Electrocatalysis. *Langmuir* **1997**, *13*, 4621−4627.

(31) Klissurski, D. G.; Uzunova, E. L. Synthesis of Nickel Cobaltite Spinel from Coprecipitated Nickel-Cobalt Hydroxide Carbonate. *Chem. Mater.* **1991**, *3*, 1060−1063.

(32) Wang, C. J.; O'Hare, D. Synthesis of Layered Double Hydroxide Nanoparticles in a Novel Microemulsion. *J. Mater. Chem.* **2012**, *22*, 21125−21130.

(33) Zhao, T.; Jiang, H.; Ma, J. Surfactant-Assisted Electrochemical Deposition of α-Cobalt Hydroxide for Supercapacitors. *J. Power Sources* **2011**, *196*, 860−864.

(34) Wang, H. L.; Hao, Q. L.; Yang, X. J.; Lu, L. D.; Wang, X. Graphene Oxide Doped Polyaniline for Supercapacitors. *Electrochem. Commun.* **2009**, *11*, 1158−1161.

(35) Villegas, J. C.; Giraldo, O. H.; Laubernds, K.; Suib, S. L. New Layered Double Hydroxides Containing Intercalated Manganese. *Inorg. Chem.* **2003**, *42*, 5621−5631.

(36) Huang, S.; Peng, H. D.; Tjiu, W. W.; Yang, Z.; Zhu, H.; Tang, T.; Liu, T. X. Assembling Exfoliated Layered Double Hydroxide (LDH) Nanosheet/Carbon Nanotube (CNT) Hybrids via Electro-

DOI: 10.1021/acsami.5b03176
ACS Appl. Mater. Interfaces 2015, 7, 19601−19610

static Force and Fabricating Nylon Nanocomposites. *J. Phys. Chem. B* **2010**, *114*, 16766−16772.
(37) Lee, J. W.; Ko, J. M.; Kim, J. D. Hierarchical Microspheres Based on α-Ni(OH)$_2$ Nanosheets Intercalated with Different Anions: Synthesis, Anion Exchange, and Effect of Intercalated Anions on Electrochemical Capacitance. *J. Phys. Chem. C* **2011**, *115*, 19445−19454.
(38) Yang, S. B.; Wu, X. L.; Chen, C. L.; Dong, H. L.; Hu, W. P.; Wang, X. K. Spherical Grown on Graphene as Advanced α-Ni(OH)$_2$ Nanoarchitecture Electrochemical Pseudocapacitor. Materials. *Chem. Commun.* **2012**, *48*, 2773−2775.
(39) Verma, S.; Joshi, H. M.; Jagadale, T.; Chawla, A.; Chandra, R.; Ogale, S. Nearly Monodispersed Multifunctional $NiCo_2O_4$ Spinel Nanoparticles: Magnetism, Infrared Transparency, and Radiofrequency Absorption. *J. Phys. Chem. C* **2008**, *112*, 15106−15112.
(40) Thomas, N.; Rajamathi, M. Intracrystalline Oxidation of Thiosulfate-Intercalated Layered Double Hydroxides. *Langmuir* **2009**, *25*, 2212−2216.
(41) Yang, G. W.; Xu, C. L.; Li, H. L. Electrodeposited Nickel Hydroxide on Nickel Foam with Ultrahigh Capacitance. *Chem. Commun.* **2008**, 6537−6539.
(42) Wei, T. Y.; Chen, C. H.; Chien, H. C.; Lu, S. Y.; Hu, C. C. A Cost-Effective Supercapacitor Material of Ultrahigh Specific Capacitances: Spinel Nickel Cobaltite Aerogels from an Epoxide-Driven Sol−Gel Process. *Adv. Mater.* **2010**, *22*, 347−351.
(43) Sing, K. S. W.; Everett, D. H.; Haul, R. A. W.; Moscou, L.; Pierotti, P. A.; Rouquérol, J.; Siemienewska, T. J. Reporting Physisorption Data for Gas/Solid Systems with Special Reference to the Determination of Surface Area and Porosity. *Pure Appl. Chem.* **1985**, *57*, 603−619.
(44) Xing, W.; Qiao, S. Z.; Ding, R. G.; Li, F.; Lu, G. Q.; Yan, Z. F.; Cheng, H. M. Superior Electric Double Layer Capacitors Using Ordered Mesoporous Carbons. *Carbon* **2006**, *44*, 216−224.
(45) Gil, A.; Montes, M. Analysis of the Microporosity in Pillared Clays. *Langmuir* **1994**, *10*, 291−297.
(46) Gil, A.; Guiu, G.; Grange, P.; Montes, M. Preparation and Characterization of Microporosity and Acidity of Silica-Alumina Pillared Clays. *J. Phys. Chem.* **1995**, *99*, 301−312.
(47) Ge, Z. H.; Li, D. Y.; Pinnavaia, T. J. Preparation of Alumina-Pillared Montmorillonites with High Thermal Stability, Regular Microporosity and Lewis/Brönsted Acidity. *Microporous Mater.* **1994**, *3*, 165−175.
(48) Ulibarri, M. A.; Labajos, F. M.; Rives, V.; Trujillano, R.; Kagunya, W.; Jones, W. Comparative Study of the Synthesis and Properties of Vanadate-Exchanged Layered Double Hydroxides. *Inorg. Chem.* **1994**, *33*, 2592−2599.
(49) Hu, C. C.; Cheng, C. Y. Anodic Deposition of Nickel Oxides for the Nickel-Based Batteries. *J. Power Sources* **2002**, *111*, 137−144.
(50) Wang, C.; Zhou, Y.; Ge, M. Y.; Xu, X. B.; Zhang, Z. L.; Jiang, J. Z. Large-Scale Synthesis of SnO_2 Nanosheets with High Lithium Storage Capacity. *J. Am. Chem. Soc.* **2010**, *132*, 46−47.
(51) Delmas, C.; Faure, C.; Borthomieu, Y. The Effect of Cobalt on the Chemical and Electrochemical Behaviour of the Nickel Hydroxide Electrode. *Mater. Sci. Eng., B* **1992**, *13*, 89−96.
(52) Morishita, M.; Ochiai, S.; Kakeya, T.; Ozaki, T.; Kawabe, Y.; Watada, M.; Tanase, S.; Sakai, T. Structural Analysis by Synchrotron XRD and XAFS for Manganese-Substituted α- and β-Type Nickel Hydroxide Electrode. *J. Electrochem. Soc.* **2008**, *155*, A936−A944.
(53) Lü, X. J.; Mou, X. L.; Wu, J. J.; Zhang, D. W.; Zhang, L. L.; Huang, F. Q.; Xu, F. F.; Huang, S. M. Improved-Performance Dye-Sensitized Solar Cells Using Nb-Doped TiO_2 Electrodes: Efficient Electron Injection and Transfer. *Adv. Funct. Mater.* **2010**, *20*, 509−515.

DOI: 10.1021/acsami.5b03176
ACS Appl. Mater. Interfaces 2015, 7, 19601−19610